

ORIGINAL ARTICLE

Transgenic expression of oncogenic BRAF induces loss of stem cells in the mouse intestine, which is antagonized by β -catenin activity

P Riemer^{1,2}, A Sreekumar^{1,2}, S Reinke², R Rad^{3,4}, R Schäfer^{1,4}, C Sers^{1,4}, H Bläker⁵, BG Herrmann² and M Morkel^{1,2}

Colon cancer cells frequently carry mutations that activate the β -catenin and mitogen-activated protein kinase (MAPK) signaling cascades. Yet how oncogenic alterations interact to control cellular hierarchies during tumor initiation and progression is largely unknown. We found that oncogenic BRAF modulates gene expression associated with cell differentiation in colon cancer cells. We therefore engineered a mouse with an inducible oncogenic BRAF transgene, and analyzed BRAF effects on cellular hierarchies in the intestinal epithelium *in vivo* and in primary organotypic culture. We demonstrate that transgenic expression of oncogenic BRAF in the mouse strongly activated MAPK signal transduction, resulted in the rapid development of generalized serrated dysplasia, but unexpectedly also induced depletion of the intestinal stem cell (ISC) pool. Histological and gene expression analyses indicate that ISCs collectively converted to short-lived progenitor cells after BRAF activation. As Wnt/ β -catenin signals encourage ISC identity, we asked whether β -catenin activity could counteract oncogenic BRAF. Indeed, we found that intestinal organoids could be partially protected from deleterious oncogenic BRAF effects by Wnt3a or by small-molecule inhibition of GSK3 β . Similarly, transgenic expression of stabilized β -catenin in addition to oncogenic BRAF partially prevented loss of stem cells in the mouse intestine. We also used BRAF^{V637E} knock-in mice to follow changes in the stem cell pool during serrated tumor progression and found ISC marker expression reduced in serrated hyperplasia forming after BRAF activation, but intensified in progressive dysplastic foci characterized by additional mutations that activate the Wnt/ β -catenin pathway. Our study suggests that oncogenic alterations activating the MAPK and Wnt/ β -catenin pathways must be consecutively and coordinately selected to assure stem cell maintenance during colon cancer initiation and progression. Notably, loss of stem cell identity upon induction of BRAF/MAPK activity may represent a novel fail-safe mechanism protecting intestinal tissue from oncogene activation.

Oncogene advance online publication, 11 August 2014; doi:10.1038/onc.2014.247

INTRODUCTION

The colon is lined by a single-layered epithelium folded into functional domains termed crypts, while the small intestine in addition contains villi that protrude into the intestinal lumen. The resulting tissue structure is highly ordered and contains a basal compartment with intestinal stem cells (ISCs) giving rise to transiently amplifying (TA) progenitor cells. These in turn differentiate into enterocytes and secretory cell types.¹ Cellular hierarchies are gradually modified during intestinal tumor initiation and progression by mutations in signaling pathways controlling homeostasis. Consequently, colon cancers can therefore exhibit gene activity characteristic for different intestinal cell types and colon cancer subtypes defined by such expression patterns differ in their therapeutic response.² It is largely unknown which oncogenic mutations modulate differentiation patterns during colon cancer progression and which constraints exist in the tumor to balance stem cell traits, proliferation and differentiation.

Colon cancer can form via different pathways, with conventional adenomas representing the most frequent benign precursor lesions. These initiate mainly, if not exclusively, via mutations

activating the Wnt/APC/ β -catenin signaling pathway in humans³ and in the mouse.^{4,5} In the normal intestine, Wnt signals are emitted in the crypt base by secretory Paneth cells and myofibroblasts and received by ISCs and in an autocrine manner by Paneth cells.¹ Wnt signals inactivate the kinase GSK3 β , resulting in stabilization of β -catenin and transcription of β -catenin/TCF4 target genes.⁶ Wnt/ β -catenin signals in the crypt are required for ISC maintenance. In line, loss of intestinal Wnt/ β -catenin signals by genetic ablation of the transcription factor TCF4 results in loss of the stem cell compartment and ultimately in loss of the intestinal epithelium in the mouse.^{7,8} In contrast, activation of β -catenin is sufficient to modulate intestinal cellular hierarchies toward adenomatous stem cell fates.⁹

Sessile serrated adenomas (SSAs) constitute a distinct class of premalignant tumors in the intestine, which are characterized by a saw-toothed and tufted tissue morphology, as well as by unique transcriptional, mutational and epigenetic patterns.^{10–12} The most prevalent mutation in human SSA is BRAF^{V600E}, representing an oncogenic alteration in the mitogen-activated protein kinase (MAPK) cascade, which is composed of consecutively activated rapidly accelerated fibrosarcoma (RAF), mitogen/extracellular

¹Laboratory of Molecular Tumor Pathology, Institute of Pathology, Charité Universitätsmedizin Berlin, Berlin, Germany; ²Department of Developmental Genetics, Max-Planck-Institute for Molecular Genetics, Berlin, Germany; ³Department of Medicine II, Klinikum Rechts der Isar, Technische Universität München, München, Germany; ⁴German Cancer Consortium (DKTK), German Cancer Research Center, Heidelberg, Germany and ⁵Department of General Pathology, Institute of Pathology, Charité Universitätsmedizin Berlin, Berlin, Germany. Correspondence: Dr M Morkel, Laboratory of Molecular Tumor Pathology, Institute of Pathology, Charité Universitätsmedizin Berlin, CCM, Chariteplatz 1, Berlin 10117, Germany.

E-mail: markus.morkel@charite.de

Received 3 March 2014; revised 19 June 2014; accepted 24 June 2014

signal-regulated kinase (MEK) and extracellular signal-regulated kinase (ERK) kinases. In the normal intestine, MAPK activity mainly relays pro-proliferative cues in the progenitor compartment of the upper crypt.¹³ BRAF-activated serrated human tumors show unique patterns of DNA methylation in CpG-rich regions^{10,14,15} and strong nuclear β -catenin staining, indicative of tumor-associated activation of the Wnt/ β -catenin pathway.^{16,17} Mice with an oncogenic BRAF^{V637E} knock-in mutation develop generalized serrated hyperplasia, thus corroborating an initiating role for oncogenic BRAF in serrated adenoma.¹⁸ Aging BRAF^{V637E} knock-in mice exhibit focal tumor progression to dysplastic serrated adenoma and metastatic carcinoma. Similar to the findings in humans, more advanced stages of murine serrated tumors showed intensified MAPK signaling and activating mutations in the Wnt/ β -catenin pathway. The specific epigenetic and mutational patterns of serrated tumors of mice and humans suggest that distinct evolutionary constraints exist in the progression of intestinal tumors that are initiated by activating BRAF mutations.

Here, we analyze a novel mouse model carrying an inducible transgene coding for human oncogenic BRAF. By analysis of intestinal tissue *in vivo* and in primary organotypic culture, we define effects of the main oncogenic driver pathways, MAPK and of Wnt/ β -catenin, on the intestinal cellular hierarchies. We could show for the first time that high levels of MAPK activity can result in the loss of the affected tissue because such signals are not compatible with the maintenance of ISC identity. We further demonstrate that ISC loss induced by MAPK can be counteracted by β -catenin activity, providing a rationale for the concomitant activation of the BRAF/MAPK and β -catenin pathways during serrated tumor progression.

RESULTS

Oncogenic BRAF activates MAPK signal transduction and modulates cell fate-associated gene expression in colon cancer cells

We tested the effects of the two colon cancer-associated mutations BRAF^{V600E} and BRAF^{V600K}¹⁹ in Caco2-tet colon cancer cells. To this end, we activated an inducible green fluorescent protein (GFP)-BRAF^{V600E} or GFP-BRAF^{V600K} in Caco2-tet cell by addition of doxycycline to the medium. We found that induction of either BRAF mutant induced the phosphorylation of the MAPK signal transducers MEK1/2 and ERK1/2, and activated transcription mediated by binding sites for the MAPK-associated transcription factor ELK to a similar extent (Figures 1a and b). Both mutations have previously been characterized as highly activating.²⁰ Transcription mediated by FOXO3 or LEF/TCF, which are associated with PI3K/AKT and Wnt/ β -catenin signal transduction, respectively,^{7,21} was not altered by either mutation.

We assessed expression of MAPK target genes by quantitative reverse transcriptase PCR (qRT-PCR) and found that both BRAF^{V600E} and BRAF^{V600K} activated *Phlda1* and *Dusp6*, whereas *Spry2* was not BRAF-responsive in Caco2-tet cells (Figure 1c). Next, we determined whether oncogenic BRAF modulates expression of *Birc5* and *Axin2*, which are highly active in stem cell-like colon cancers, as well as *Muc2* and *Krt20*, which are active in Goblet cell-like colon cancers.² We found that *Birc5* and *Axin2* were gradually inhibited by increasing amounts of BRAF^{V600E} or BRAF^{V600K}, whereas *Muc2* and *Krt20* were progressively activated (Figures 1d and e). These results suggest that activation of the BRAF/MAPK signaling axis can affect cell fate-associated transcriptional activity in colon cancer cells and thus may modulate cell differentiation choices during intestinal tumor initiation and progression.

Transgenic expression of oncogenic BRAF induces intestinal serration

To study the effects of oncogenic BRAF on cell hierarchies in the intestinal epithelium, we engineered an inducible transgene for

the human oncogene BRAF^{V600K} linked to the fluorescent protein tdTomato into a modified Gt(ROSA26)Sor locus²² of murine embryonic stem cells and derived transgenic mice by diploid aggregation (Figure 2a). In transgenic mice, BRAF^{V600K} expression in the intestine was induced by administration of doxycycline via the drinking water. We were able to induce BRAF^{V600K} in transgenic mice for up to 4 days before they showed signs of distress and had to be killed.

In the non-induced state, the small intestine of transgenic mice displayed regular architecture and a smooth epithelial surface with cylindrical enterocytes admixed with Goblet cells. Paneth cells, as identified by eosinophilic cytoplasmic granules, were restricted to the bases of the crypts. Significant morphologic alterations were found after 3 and 4 days of BRAF^{V600K} induction (Figure 2b, Supplementary Figure 1). The villus surface became saw-toothed, and tufts of aggregated enterocytes were seen at the villus tip. Basal positioning of nuclei in the epithelium was lost, nuclei were enlarged and the nucleus to cytoplasm ratio was increased. The contact surface of the cells to the basal membrane often appeared to be narrowed, resulting in a hobnail appearance of the cells and the presence of dis cohesive cell clusters. Paneth cells lost their strict location at the base of the crypt and were also found at more luminal positions. We frequently observed the formation of rounded glands at crypt-to-villus junctions, which contained Paneth cells. We also found that maturation of secretory lineages was perturbed, and we frequently observed intermediary cells that expressed both Goblet and Paneth cell markers (Supplementary Figure 2).

In the large intestine changes were similar, yet less pronounced (Figure 2b, Supplementary Figure 3). We observed generalized Goblet cell-rich epithelial serration with widened luminal openings of crypts. Similar to the surface alterations in the small bowel, tufts of clustered cells projected into the lumen. Associated with the widening of crypts and luminal openings, the submucosal space between the epithelium and the muscularis appeared reduced to only few visible fibroblasts.

Transgenic expression of oncogenic BRAF induces MAPK hyperactivation in the intestinal epithelium

We analyzed transgene expression and resulting changes in MAPK cascade activity in the intestinal epithelium by western blots and immunohistochemistry (IHC) (Figure 2c, Supplementary Figures 4 and 5). We detected low levels of endogenous RAF proteins in the intestinal epithelium of non-induced mice, while transgenic BRAF^{V600K} contributed to a more pronounced RAF signal in induced mice. In line, only low levels of the phosphorylated active forms of MEK and ERK were present in non-induced mice, but phosphorylation was stronger in induced animals. We compared phospho-MEK1/2 and phospho-ERK1/2 levels in the intestinal epithelium of induced mice with levels found in the human colon cancer cell lines RKO and HT29, which both harbor a BRAF^{V600E} mutation. MEK1/2 and ERK1/2 showed activity levels of various strengths in the intestinal epithelia of mice and in cell lines. Phosphorylated ERK1/2 was most strongly elevated in RKO cells. These western blot analyses demonstrate that transgenic BRAF^{V600K} induces MAPK activity in the intestine of mice to levels comparable, but not exceeding those found in human colon cancer cell lines.

Phospho-Mek1/2 and phospho-ERK1/2 signals were generalized in all compartments spanning crypt bases to villus as assessed by IHC (Supplementary Figures 4 and 5). However, the proliferative zones were only slightly expanded after BRAF^{V600K} induction in both small and large intestine (Supplementary Figure 6). We used qRT-PCR to quantify expression of well-known MAPK target genes in the intestine and found strong induction (Figure 2d), comparable to that seen in foci of dysplastic progression in mice harboring a knock-in allele of oncogenic

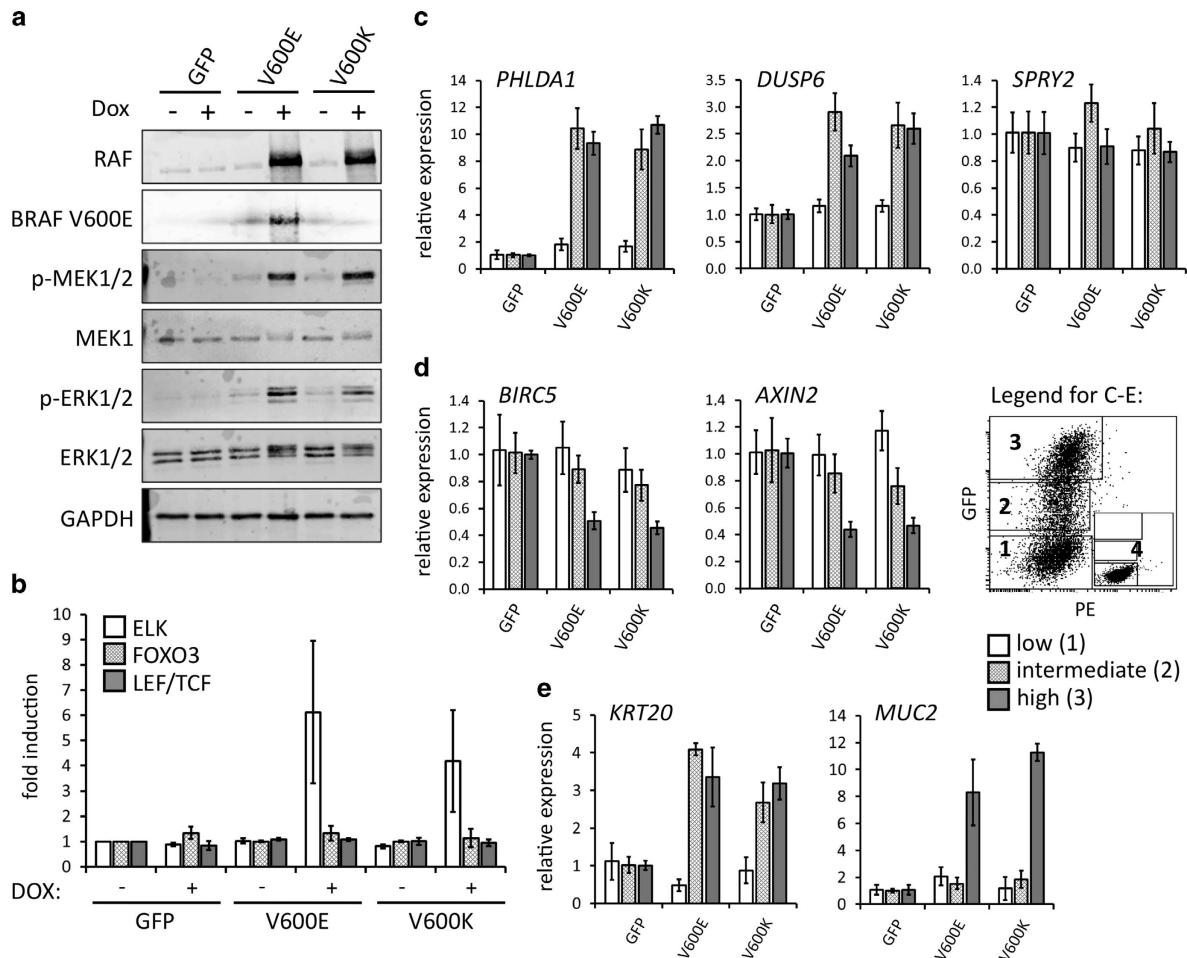


Figure 1. Oncogenic BRAF^{V600E} and BRAF^{V600K} activate MAPK signal transduction, ELK activity and modulate cell fate-specific gene expression in colon cancer cells. **(a)** Western blot analysis of non-induced and 24 h induced Caco2-tet BRAF^{V600E} and BRAF^{V600K} human colon cancer cells, using antibodies directed against RAF, BRAF(V600E), MEK1, phospho-MEK1/2, ER1/2 phospho-ERK1/2 and glyceraldehyde 3-phosphate dehydrogenase (GAPDH) as a loading control. **(b)** Reporter assays in non-induced and 24h induced Caco2-tet BRAF^{V600E} and BRAF^{V600K} human colon cancer cells, using luciferase reporters containing multimerized ELK, FOXO3 or LEF/TCF binding sites. **(c–e)** qRT-PCR analyses of gene expression in induced Caco2-tet GFP, GFP-BRAF^{V600E} and GFP-BRAF^{V600K} cells. Before analyses, cells were sorted according to transgene expression. FACS plot in legend: windows 1–3 denote low, intermediate and high transgene-expressing populations. Inset 4 displays untransfected Caco2-tet cells. **(c)** Analysis of MAPK target genes. **(d)** Analysis of marker genes for SC-like colon cancer. The intestinal SC marker genes *LGR5* and *OLFM4* had too low expression to call in Caco2-tet cells. **(e)** Analysis of marker genes for Goblet-like colon cancer.

BRAF^{V637E}¹⁸ MAPK target genes were activated in both crypts and villi of BRAF^{V600K}-induced mice (Supplementary Figure 7).

Transgenic expression of oncogenic BRAF causes loss of ISCs

We next analyzed the effects of amplified MAPK signal transduction on the intestinal crypt, which contains ISCs and is essential for tissue maintenance. In control mice, ISCs and secretory Paneth cells were both restricted to the crypt base, as assessed by RNA *in situ* hybridization for *Olfm4*²³ and Lysozyme IHC, respectively (Figure 3a and Supplementary Figure 4). *Olfm4*-positive ISCs had characteristic wedge-like shapes and were mostly proliferative, as shown by Ki67 staining. In striking contrast to non-induced controls, crypts of BRAF^{V600K}-induced mice displayed only very weak *Olfm4* signals already 3 days after induction, suggesting an exhaustive loss of ISCs. Ki67-positive proliferative cells were frequently found at the crypt base. However, these did not have the characteristic shape of ISCs, but were round to cylindrical, resembling proliferative cells of the TA zone. Furthermore, Lysozyme-positive Paneth cells were displaced from the crypt

base and strongly positive in Periodic acid-Schiff (PAS) staining, resembling Goblet cells and confirming our previous analyses (see Supplementary Figure 2 above).

To ascertain the loss of ISCs in crypts upon transgenic BRAF^{V600K} induction, we analyzed the expression of several ISC marker genes²³ by qRT-PCR and found all markers strongly reduced in the induced intestines (Figure 3b).

To quantify the fraction of ISCs in normal versus BRAF-induced crypts, we mated BRAF^{V600K} transgenic and firefly luciferase/tdTomato-transgenic control mice to Lgr5-EGFP stem cell-marking reporter mice.²⁴ Using fluorescence-activated cell sorting (FACS), we found that crypt cell suspensions isolated from control mice contained between 3 and 8% of enhanced GFP (EGFP)-positive stem cells, while crypt cell suspensions isolated from BRAF^{V600K} transgenic mice induced for 3 days contained <0.2% EGFP-positive ISCs (Figure 3c).

Transgenic expression of oncogenic BRAF promotes TA cell generation combined with ISC depletion

In order to elucidate the fate of ISCs upon BRAF^{V600K} induction, we first evaluated end points of apoptotic and senescence programs,

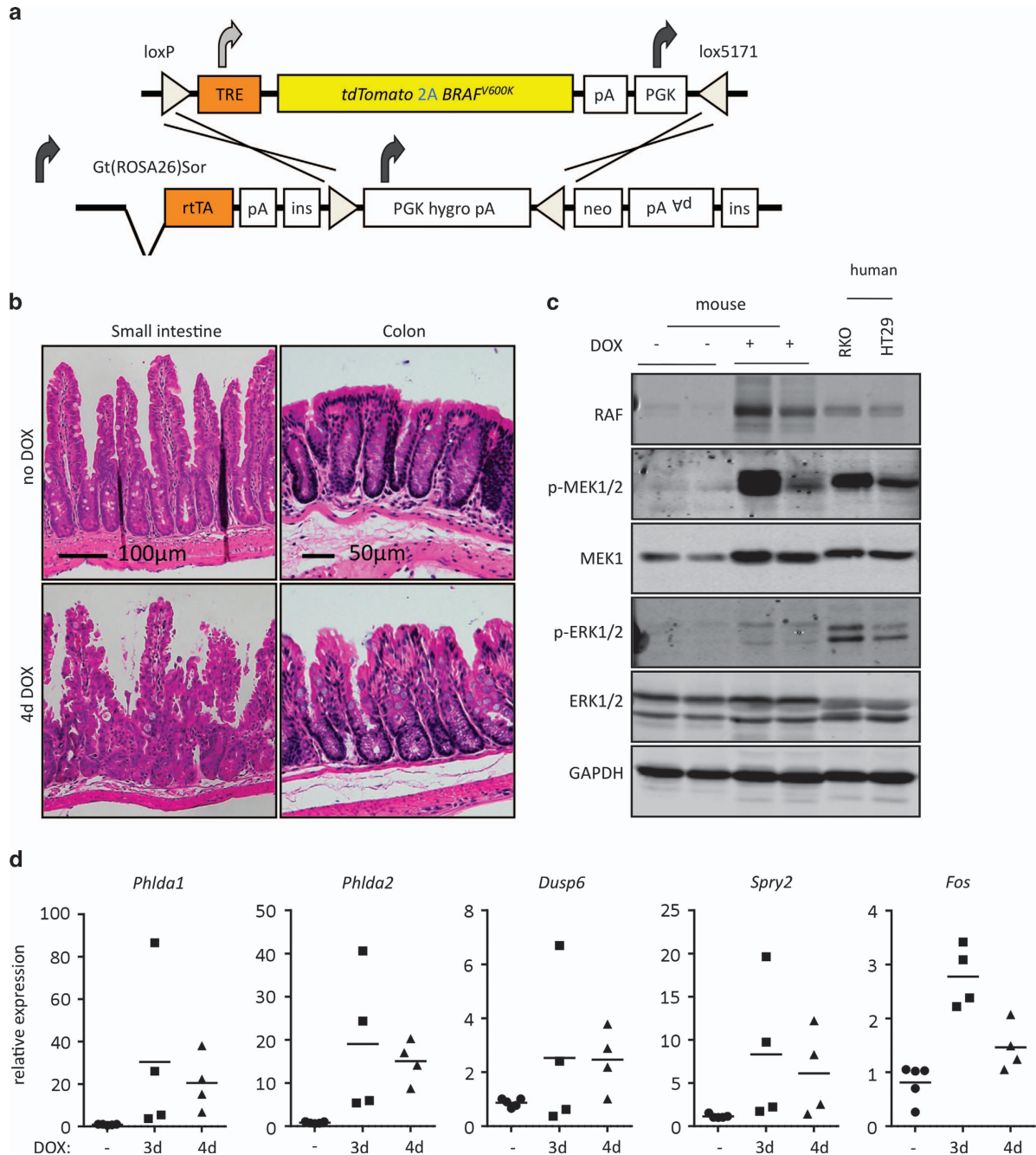


Figure 2. Transgenic BRAF^{V600K} induces MAPK activity and serration in the intestinal epithelium. **(a)** Scheme of the transgene system used for an inducible transgenic expression. For further details, see Vidigal *et al.*²² **(b)** Overview of tissue morphology after 4 days of transgenic BRAF^{V600K} induction, hematoxylin–eosin-stained paraffin sections are shown. For further detailed images, see Supplementary Figure 1. **(c)** Western blot analysis of purified epithelium of non-induced and 3-day induced mice and human colon cancer cell lines carrying a BRAF^{V600E} mutation, using antibodies directed against RAF, MEK1, phospho-MEK1/2, ERK1/2 phospho-ERK1/2 and glyceraldehyde 3-phosphate dehydrogenase (GAPDH) as a loading control. **(d)** Expression of the MAPK target genes *Phlda1*, *Phlda2*, *Dusp6*, *Spry2* and *Fos* in intestines of non-induced, 3- and 4-day induced mice, as assessed by qRT-PCR.

which can be triggered as a response to BRAF.^{25,26} We found that induction of BRAF^{V600K} induced significant DNA damage in the intestine, as demonstrated by immunofluorescence analysis of phosphorylated histone γ H2A. However, we did not find increased apoptosis in BRAF^{V600K}-induced intestinal tissues, as assessed by cleaved caspase 3 IHC (Supplementary Figure 8). Similarly, oncogene-induced senescence was not observed, as indicated by lack of staining for senescence-associated β -galactosidase (Supplementary Figure 9).

We next analyzed gene expression in BRAF^{V600K}-induced ISCs, using tdTomato-BRAF^{V600K};Lgr5-EGFP or control tdTomato-luc;Lgr5-EGFP compound transgenic mice. For this, we sorted cells displaying both red and green fluorescence, marking activity of the BRAF^{V600K} or control transgenes and the Lgr5-EGFP stem cell-specific reporter, respectively. As almost no double-positive cells were detected 2 or 3 days after BRAF^{V600K} induction (see Figure 3c and data not shown), we induced the BRAF^{V600K} transgene for only 24 h, and could isolate sufficient numbers of

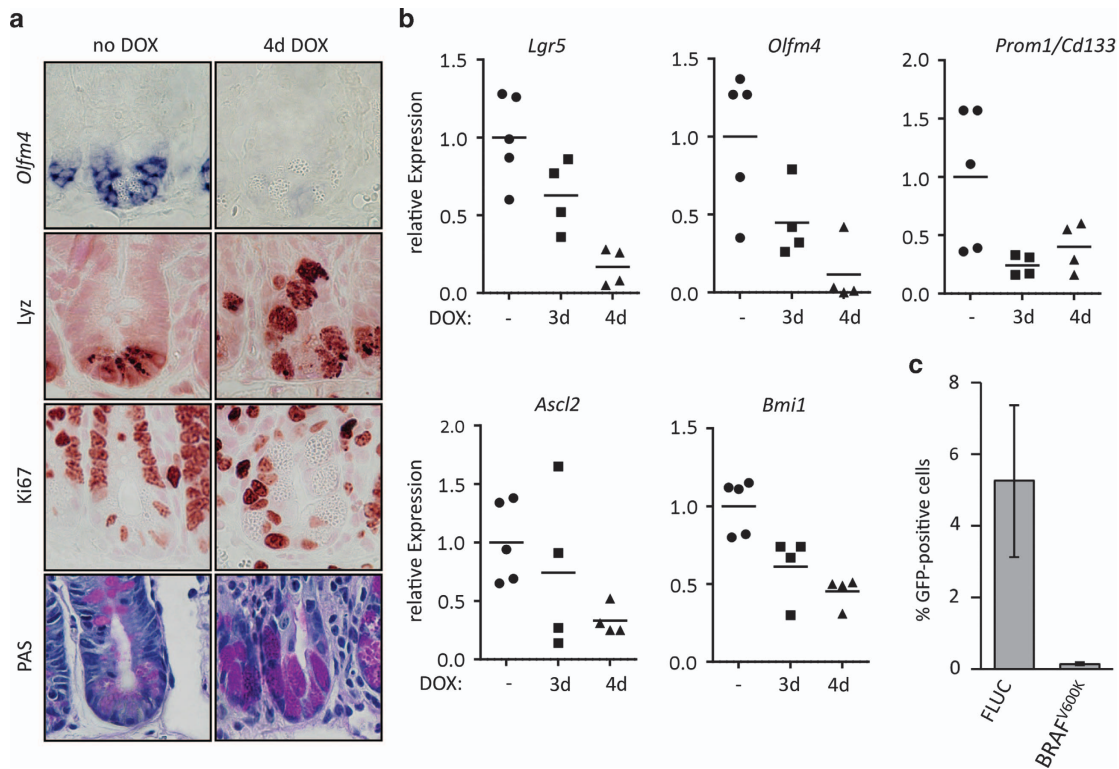


Figure 3. Transgenic BRAF^{V600K} induces loss of ISCs. **(a)** Visualization of ISCs (*Olfm4* RNA *in situ* hybridization), proliferative cells (Ki67 IHC), Paneth cells (Lysozyme IHC) and Goblet cells (Periodic acid-Schiff staining) in crypts of non-induced and BRAF^{V600K}-induced mice. **(b)** Expression of ISC marker genes *Lgr5*, *Olfm4*, *Prom1/Cd133*, *Ascl2* and *Bmi1*²³ in intestines of non-induced, 3- and 4-day induced mice, as assessed by qRT-PCR. **(c)** FACS analysis of crypt cell suspensions isolated from induced compound transgenic mice carrying an *Lgr5*-EGFP stem cell reporter gene²⁴ and an inducible tdTomato/BRAF^{V600K} or tdTomato/firefly (FLUC) luciferase control transgene.

double-fluorescent cells by FACS, along with single-fluorescent and non-fluorescent cell populations. Expression profiles of sorted cells were analyzed by microarrays. As expected, MAPK target genes such *Areg*, *ler3* and *Tnfrsf12a*, as well as the MAPK targets and feedback inhibitors *Dusp4*, *Dusp6*, *Spry2* and *Spry4* were strongly activated in ISCs following BRAF^{V600K} induction (Figure 4a). We also identified many novel BRAF target genes in the intestine, prominently among these the putative signal transducer gene *Anxa10*, which has recently been identified as a specific marker for SSA in human patients²⁷ (Figures 4b and c).

We used gene set enrichment analysis²⁸ to analyze activities of gene expression programs in the sorted ISCs (Figure 4d). We evaluated gene signatures comprising MAPK or β -catenin target genes, as well as signature genes enriched in stem cells or proliferative committed TA cells of the intestinal epithelium.^{29–32} As expected, we found that a signature of MAPK target genes was strongly induced by BRAF^{V600K} in ISCs when compared with luciferase-expressing control ISCs. However, signatures of β -catenin target genes were not significantly changed. Strikingly, we found a strongly activated signature of proliferative TA cells in the BRAF^{V600K}-induced sorted *Lgr5*-EGFP-positive cells, while the ISC signature was not significantly altered at this early time point after transgene induction (Figure 4d and Supplementary Figure 10). Taken together, these findings show that ISC and TA cell gene expression programs are both active side by side in the BRAF^{V600K}-expressing ISCs 24 h after induction, and the latter is strongly enhanced. Our gene expression data thus confirm and extend the morphological analyses, and suggest that ISCs rapidly and collectively convert to committed TA progenitors after BRAF^{V600K} induction. Furthermore, secretory lineages are perturbed and intermediate secretory cells emerge (for a model of the resulting crypt cell types, see Figure 4e).

Effects of oncogenic BRAF in organotypic culture can be rescued by MEK inhibition

To follow tissue development and signal transduction in the intestinal epithelium after BRAF^{V600K} induction in more detail, we took advantage of organotypic primary tissue culture.³³ We were unable to establish organoids from intestines of mice induced for BRAF^{V600K} expression for 3 or 4 days, further supporting our finding that ISCs are lost by the treatment. Organoids prepared from non-induced BRAF^{V600K} transgenic mice that were maintained without doxycycline were organized into radial crypts and a central differentiated villus domain containing debris of extruded cells, as expected. Upon BRAF^{V600K} induction, organoids underwent rapid changes: crypts became progressively wider and shallower, until they were indistinguishable from the central villus tissue (Figure 5a). Time-lapse photography revealed rapid development of an irregular and highly motile apical epithelial surface and frequent loss of Paneth cell localization (data not shown). Sections of induced organoids frequently displayed serration, reminiscent of the morphological changes observed *in vivo* (Supplementary Figure 11). These induced organoids showed a markedly reduced expression of crypt domain markers, such as for the stem cell markers *Lgr5*, *Olfm4* and *Cd44*, the Paneth cell marker *Mmp7*, the Wnt target gene *Axin2* and for the Goblet cell marker *Muc2*. In contrast, expression of the villus enterocyte marker *Fabp2* was not significantly altered (Figure 5b). Within 1–2 days of induction, organoids lost all structure and disintegrated. These data are in agreement with the *in vivo* analyses, and validate that following BRAF^{V600K} induction epithelial serration is induced and ISCs are lost in a tissue-intrinsic manner. In addition, we also observed loss of the proliferative compartment, which probably can no longer be maintained in the absence of stem cells and after

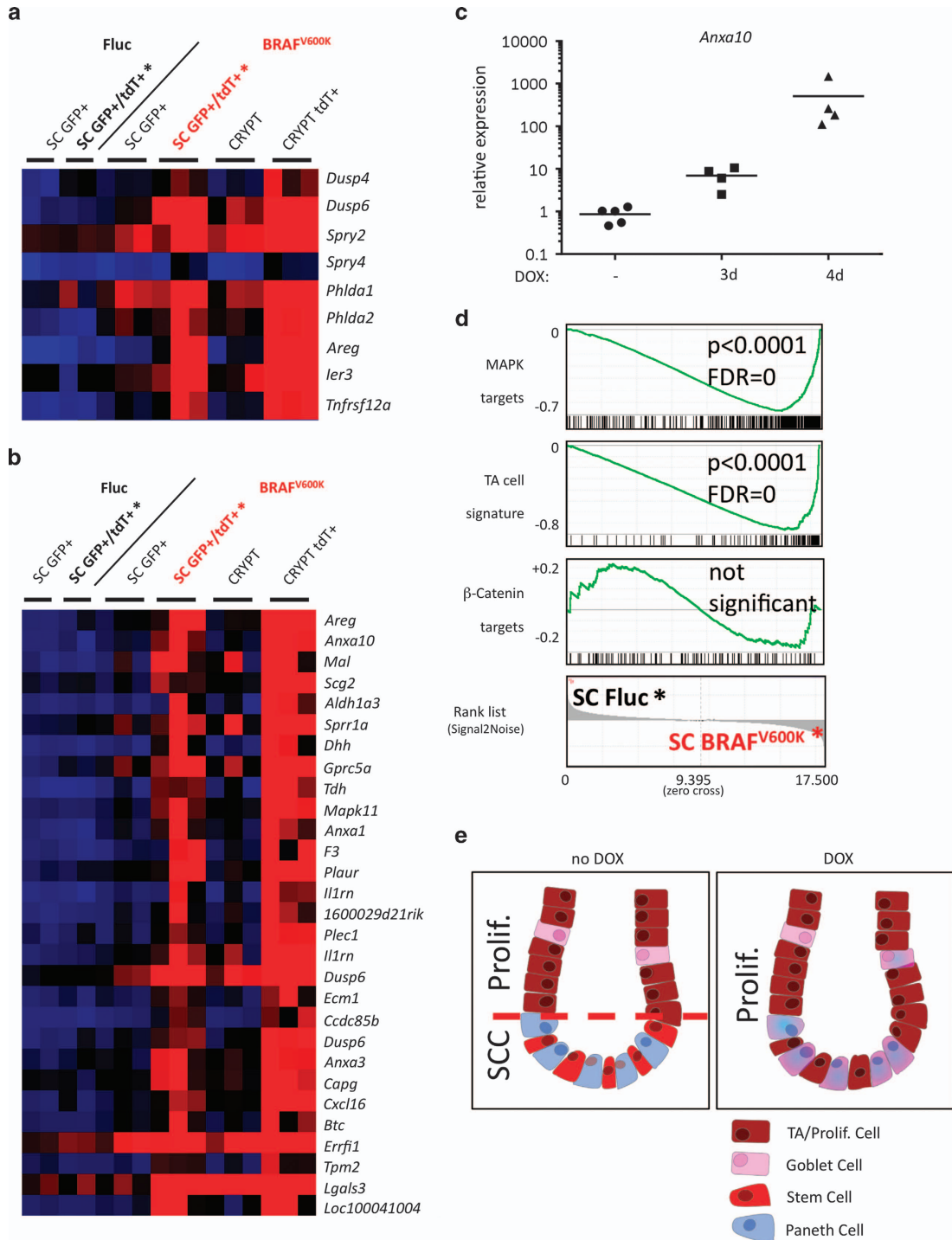


Figure 4. Transgenic BRAF^{V600K} induces MAPK activity and TA cell-specific gene expression programs in ISCs. **(a)** Gene expression in sorted crypt cell populations of BRAF^{V600K}-induced and luciferase-induced control mice. Expression of MAPK target genes is shown (MAPK targets selected from Rad *et al.*¹⁸). Color code is red for high relative expression, blue for low relative expression. Mouse transgenes and cell populations are indicated on top of figure. 'SC GFP+' indicates (stem cell) populations positive for green fluorescence of the Lgr5-EGFP reporter, 'CRYPT' indicates populations negative for green fluorescence, 'tdT+' indicates populations that were sorted for fluorescence of the tdTomato (linked to BRAF^{V600E} or firefly luciferase) transgene. **(b)** Expression of genes strongly induced by transgenic BRAF^{V600E}. Color code is as in **a**. **(c)** Expression of *Anxa10*, a specific marker gene of SSA, as assessed by qRT-PCR, 3 and 4 days after BRAF^{V600E} induction in the intestine. **(d)** Gene set enrichment analysis (GSEA) analysis of stem cell populations isolated from BRAF^{V600E}-induced versus firefly luciferase control transgenic mice. Gene signatures of MAPK target genes,²⁹ TA cell-enriched genes³² and β -catenin target genes³¹ are shown. Analysis of further β -catenin target genes³⁰ and a stem cell-specific signature³² can be found in the Supplementary Figure 10. Enrichment score graphs (top, green), signature gene distributions (black lines below ES curves), *P*-values and false discovery rates (FDRs) are given. Significance cutoffs were $P < 0.05$, FDR < 0.25. **(e)** Schematic representation of cell types in the crypts before and after BRAF^{V600K} induction.

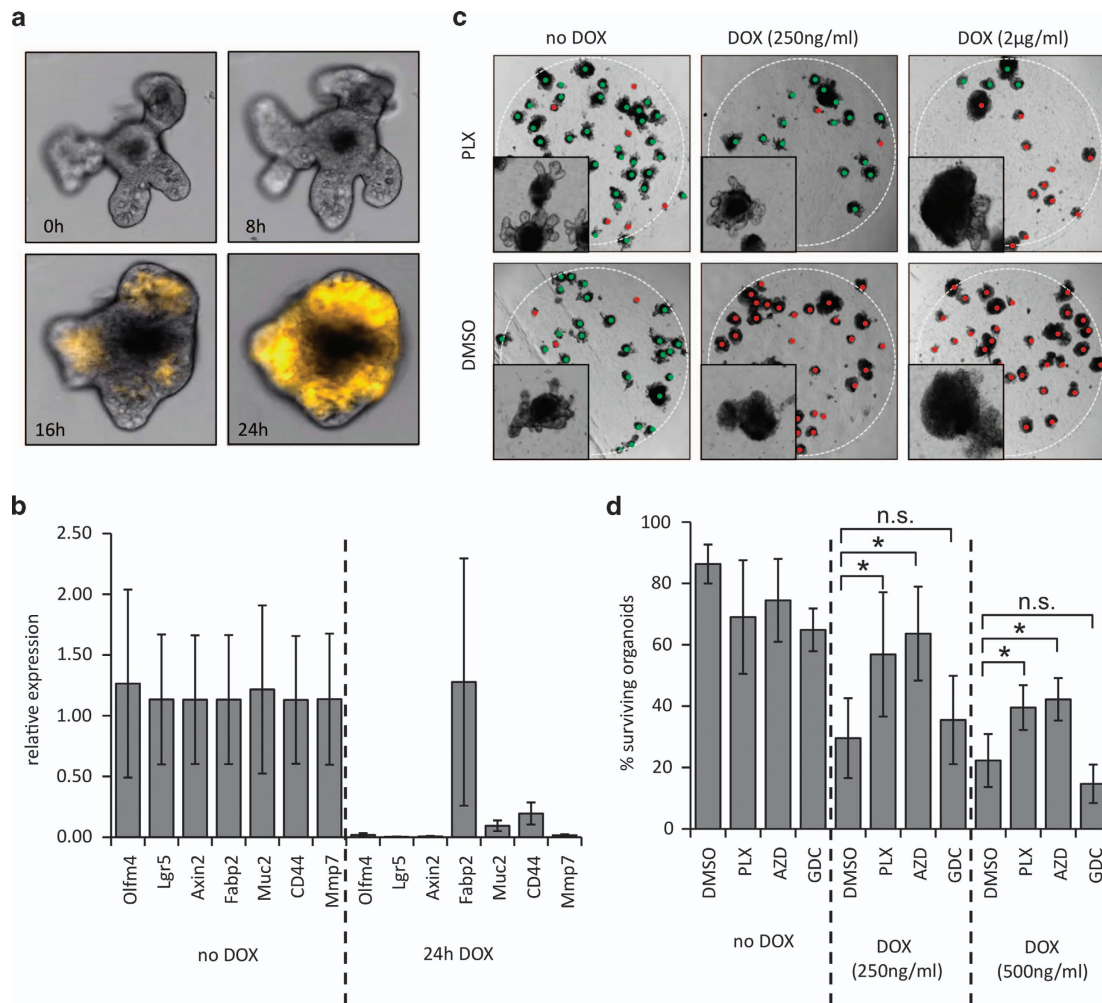


Figure 5. Transgenic BRAF^{V600K} results in a MAPK-dependent loss of crypt domains in organotypic culture. **(a)** Stills from time-lapse microscopy of BRAF^{V600K}-induced organoids. Time span since induction is given in panels. Yellow overlay indicates fluorescence of the tdTomato-2A-BRAF^{V600K} transgene. **(b)** qRT-PCR analysis of marker gene expression in non-induced versus BRAF^{V600K}-induced organoids, 24 h after induction with 2 μg/ml doxycycline. **(c, d)** The BRAF^{V600E} inhibitor PLX4720 and the MEK1/2 inhibitor AZD6244 rescue organoids from deleterious effects of transgenic BRAF^{V600K}. **(c)** Microscopic images of organotypic cultures, 24 h after addition of doxycycline and/or PLX4720, as indicated. Green dots mark intact organoids, red dots mark disintegrated organoids. **(d)** Quantification of organoid survival 36 h after BRAF^{V600K} transgene induction with doxycycline in the presence or absence of small-molecule inhibitors. DMSO: solvent control; PLX: PLX4720 (42 μM); AZD: AZD6244 (8 μM); GDC: GDC0941 500 nM). *n* ≥ 4 wells in multiple experiments, significance calculated by Student's *t*-test. **P* < 0.005, else NS (not significant).

loss of crypt topology. The enhanced disintegration of the tissue architecture *in vitro* can likely be attributed to the lack of supporting effects from the surrounding tissues, which are an important source for growth factors *in vivo* but are lacking in organotypic culture.³⁴

In order to dissect signaling cascades downstream of oncogenic BRAF, we treated organotypic cultures with small-molecule inhibitors. In a series of proof-of-principle experiments, we first assessed the effects of PLX4720,³⁵ a specific inhibitor of BRAF^{V600E} and possibly other oncogenic forms of BRAF. In non-induced organotypic cultures, PLX4720 did not cause any effects. When BRAF^{V600K} was induced using a low concentration of doxycycline, PLX4720-treated cultures preserved crypt/villus topology and survived for several days, indicating inhibition of BRAF^{V600K} by PLX4720 (Figures 5c and d). Under these conditions, PLX4720 also suppressed the strong activation of the MAPK target genes *Fos* and *Dusp6* that were induced by BRAF^{V600K} (Supplementary Figure 12). To establish whether increased MAPK activity is causative for the loss of ISCs and crypts, we inhibited the downstream MEK1/2

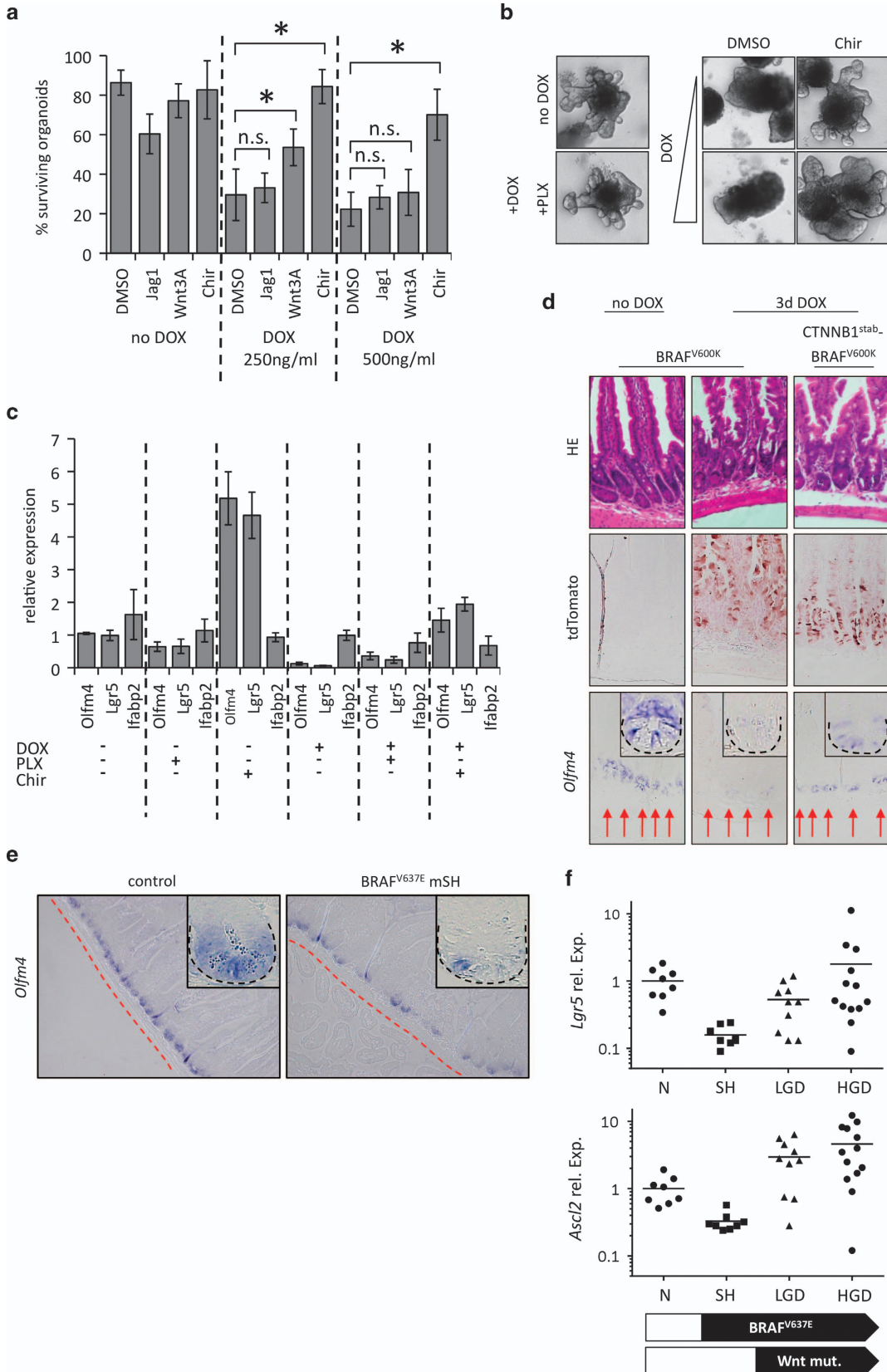
kinases using AZD6244³⁶ and alternatively the phosphatidylinositol 3 kinase cascade using the specific inhibitor GDC0941.³⁷ Significantly, MEK inhibition by AZD6244 had a similar protective effect as PLX4720 and supported organoid survival in the presence of doxycycline (Figure 5d). In contrast, inhibition of the phosphatidylinositol 3 kinase cascade by GDC0941 did not rescue organoid survival. These results indicate that oncogenic signals causing serration and loss of ISCs are transduced via activation of the MAPK cascade.

Activation of Wnt/β-catenin signaling rescues ISC loss after induction of oncogenic BRAF

In our mouse model, induction of transgenic BRAF^{V600K} resulted in strong MAPK signal activation and in epithelial serration, yet also in loss of ISCs. As the ISC compartment is maintained by Wnt and Notch signals,¹ we tested the effects of the ligands Wnt3a and Jagged1, which are known to activate the Wnt and Notch pathways in organotypic culture.³³ We found that Wnt3a, but not

Jagged1, led to a partial rescue of organoid integrity (Figure 6a). Furthermore, we used the selective GSK3 β -inhibitor CHIR99021,³⁸ which stabilizes β -catenin.³⁹ In organotypic culture, CHIR99021

was tolerated and resulted in a visible expansion of crypt domains after 2 days, probably due to the induction of ectopic β -catenin activity that is normally restricted to the crypt base (Figure 6b).



Remarkably, when we induced BRAF^{V600K} in cultures, inhibition of GSK3 β by CHIR99021 resulted in a substantial rescue of crypt-villus architecture and in organoid survival (Figures 6a and b). We observed that even when BRAF^{V600K} was strongly induced by high levels of doxycycline, GSK3 β inhibition resulted in the survival of many organoids. Their crypt domains persisted while becoming enlarged and hyperplastic. In agreement with the changes in organoid architecture observed, we found that CHIR99021 strongly activated the ISC marker genes *Lgr5* and *Olfm4*, and that this activation was strong even in the presence of induced BRAF^{V600K} (Figure 6c).

We have previously shown that transgenic expression of stabilized β -catenin promotes stem cell identity in intestinal epithelium.⁹ We therefore asked whether activation of β -catenin signaling could rescue the stem cells loss caused by transgenic BRAF^{V600K} *in vivo*. To this end, we engineered a triple transgene into an inducible Gt(ROSA26)Sor locus, consisting of tdTomato, BRAF^{V600K} and stabilized β -catenin. We found that BRAF^{V600K}/ β -catenin^{stab} compound transgenic mice also develop serration. Importantly, and in contrast to the BRAF^{V600K} mice analyzed before, we observed the presence of many residual *Olfm4*-positive ISCs 3 days after transgene induction (Figure 6d). Taken together, our experiments demonstrate that enhanced Wnt/ β -catenin pathway activity can strongly reduce the loss of ISCs *in vitro* and *in vivo*, caused by BRAF^{V600K}-induced MAPK hyperactivation.

Finally, we analyzed ISCs in a murine tumor progression model, based on knock-in of a BRAF^{V600E} homolog¹⁸ (Figure 6e and Supplementary Figure 13). These mice display serrated intestinal hyperplasia upon oncogenic activation of BRAF, and develop progressive dysplastic foci that frequently contain activating mutations in the Wnt/ β -catenin pathway in addition to the initiating oncogenic BRAF. When visualizing ISCs by *Olfm4 in situ* hybridization, we found that BRAF-activated hyperplastic intestines showed diffuse and scattered signals in neighboring crypts, whereas intestines of control mice displayed a continuous band of *Olfm4*-positive crypts. We also observed a strong reduction of mature Paneth cells, as assessed by Lysozyme IHC. We next used qRT-PCR to assess expression levels of the ISC markers *Lgr5* and *Ascl2* during the different stages of tumor progression in BRAF^{V637E} mice (Figure 6f). We found that hyperplastic intestines showed a marked reduction of expression for both *Lgr5* and *Ascl2* relative to non-recombined control intestines. In contrast, progressive dysplastic foci that frequently contain Wnt/ β -catenin mutations displayed an increase in ISC marker expression. These data support and extend our previous results, suggesting that an initiating BRAF mutation can reduce the ISC pool, whereas enhanced Wnt/ β -catenin signals expand the ISC pool at later stages of serrated intestinal tumor progression.

DISCUSSION

We report a novel oncogene mouse model that is based on conditional activation of transgenic BRAF^{V600K}. Induced mice showed generalized serration of the intestinal epithelium, combined with strong reduction of the ISC pool.

Transgenic induction of oncogenic BRAF rapidly induced a phenotype that displayed striking parallels to SSA in the human colon. In particular, the mouse model showed a serrated epithelial morphology, tufting of cells at the luminal borders, reduction of the interluminal mesenchymal tissue and widening of the colonic crypts,⁴⁰ which are all features of human SSA. We therefore conclude that activation of MAPK signaling by oncogenic BRAF is sufficient to induce multiple pathognomonic features of SSA. We furthermore noticed a high extent of cellular atypia (that is, a high nucleus-to-cytoplasmic ratio) normally associated with later stages of serrated tumor progression in humans.

Transgenic expression of BRAF^{V600K} in the intestinal epithelium converted stem cells collectively into proliferative TA cells. The resulting ISC depletion was counteracted by upregulation of Wnt/ β -catenin signaling by Wnt3a ligand or by small-molecule inhibition of GSK3 β in organotypic culture, or by transgenic expression of stabilized β -catenin in the mouse intestine. Both high MAPK and β -catenin activity has been noted in human SSA^{16,17} and in BRAF-driven serrated intestinal tumors in the mouse.¹⁸ Our data suggest that the concomitant activation of MAPK and β -catenin could be required to assure stem cell and consequently tumor tissue maintenance during progression of SSA, and our ISC marker analysis during serrated tumor progression in the mouse is in agreement with such a model.

The transgenic mouse model presented here expresses BRAF^{V600K} to an extent that exceeds endogenous BRAF transcript or protein levels in normal intestinal cells (for quantification of transgene expression, see Figure 2c and Supplementary Figure 14). This is in contrast to previous mouse models of oncogenic activation of BRAF, which used knock-in alleles.^{18,26} As a consequence, BRAF^{V600K} induction in our mouse model results in immediate and strong activation the MAPK cascade. Consequently, MAPK target genes in transgenic BRAF^{V600K} mice were induced to levels characteristic of more advanced stages of tumor progression obtained in BRAF^{V637E} knock-in mice.¹⁸ Mechanisms of how MAPK signals are further intensified in serrated intestinal tumors of mice and humans after the initial BRAF mutation remain to be further defined. It is of note that amplification of oncogenic BRAF has been found in colon cancer cell lines that were resistant to MEK inhibition⁴¹ and also in BRAF-mutant human colorectal cancer,⁴² demonstrating that high levels of oncogenic BRAF are tolerated in more advanced tumor stages.

Figure 6. β -Catenin activity antagonizes loss of ISCs induced by oncogenic BRAF. **(a, b)** Quantification of survival of BRAF^{V600K} transgenic organotypic cultures, after induction with 250 ng/ml, 500 ng/ml or 2 μ g/ml of doxycycline and the following growth factors and inhibitors: Jagged1 peptide (1 μ M), Wnt3a peptide (100 ng/ml), CHIR99021 (6 μ M), PLX4720 (42 μ M). **(a)** Quantification of organoid survival in $n \geq 4$ wells in multiple experiments, significance calculated by Student's *t*-test. **P* < 0.005, else NS (not significant). **(b)** Images of representative organoids 36 h after DOX and/or inhibitor supplementation, as indicated. **(c)** Expression of the stem cell marker genes *Olfm4* and *Lgr5*, and of the villus enterocyte marker gene *Fabp2* in organoid cultures, 24 h after induction with 500 ng/ml doxycycline, and/or treatment with 42 μ M PLX4720 or 6 μ M CHIR99021, as indicated. **(d)** Partial rescue of *Olfm4*-positive ISCs *in vivo* by transgenic stabilized β -catenin 3 days after transgene induction. Hematoxylin and eosin (HE) stainings (top panels), IHC for tdTomato (transgene induction, middle panels) and *Olfm4* RNA *in situ* hybridization (ISC visualization, lower panels) are given. Red arrows point to crypt bases, insert shows magnification of representative crypts (lower panels). Compositions of transgenes are given above. **(e, f)** Analysis of ISCs in a mouse model of serrated tumor progression, initiated by BRAF^{V637E}.¹⁸ **(e)** Visualization of ISCs by *Olfm4* RNA *in situ* hybridization in control and BRAF^{V637E} hyperplastic intestines. Red line indicates crypt level. Inserts show magnification of individual crypts. It is of note that crypts of BRAF^{V637E} are often strongly variegated. For further images, see Supplementary Figure 13. **(f)** Expression of ISC marker genes *Lgr5* and *Ascl2*²³ in normal (N) and serrated hyperplastic (SH) intestines, as well as in low-grade (LGD) and high-grade (HGD) dysplastic progressive foci, as assessed by qRT-PCR. Arrows below indicate the progression model,¹⁸ with BRAF^{V637E} inducing sustained hyperplasia and Wnt/ β -catenin mutations leading to dysplastic progression.

Oncogenic forms of KRAS and BRAF are mutually exclusive drivers of oncogenic progression in human colon cancer. Although both oncogenes activate the MAPK cascade, differences also exist: first, KRAS activates a number of further signal transducers in addition to BRAF,⁴³ and second, oncogenic KRAS, but not BRAF, is subject to strong additional feedback control within the MAPK cascade.⁴⁴ These differences may explain why BRAF-mutated tumors have distinct molecular features and therapeutic profiles compared with BRAF non-mutated tumors, including those that are KRAS mutated.³ Similar to BRAF, oncogenic KRAS can also initiate serrated lesions in the mouse,⁴⁵ but in contrast to BRAF, tumor progression in KRAS-transgenic mice crucially depends on loss of the tumor-suppressor Ink4a/ARF, but not on Wnt/ β -catenin activation. The KRAS and BRAF oncogenes may also have contrasting effects on cellular hierarchies in the intestine, as oncogenic KRAS in combination with loss of APC can induce ectopic stem cells in the mouse intestine,⁴⁶ and KRAS mutations produced cells that favor ISC over TA cell fate and thus spread within individual crypts.⁴⁷ In contrast, our results suggest that oncogenic activation of BRAF would support the adoption of TA over ISC cell fate, which would result in preferential exclusion from the stem cell pool and clonal elimination. However, this assumption has not been tested on a clonal basis here.

Wnt and MAPK signaling have been shown to co-operate during conventional intestinal tumor progression, with APC/ β -catenin pathway mutations occurring first: nuclear localization of β -catenin and expression of cancer stem cell markers after loss of APC are increased by mutational activation of the MAPK-controlling GTPase KRAS,^{48,49} and in turn KRAS can be stabilized by β -catenin activity.⁵⁰ In contrast, activation of MAPK signaling downstream of oncogenic BRAF can inhibit β -catenin effects in melanoma.⁵¹ Therefore, interactions between the two signaling cascades may be highly cell type- and context-specific.⁵² To assess whether BRAF/MAPK activation may immediately alter transcription of β -catenin target genes during serrated tumor development, we analyzed FAC-sorted residual ISCs after short-term induction of BRAF^{V600K} by microarrays, but found no immediate changes in β -catenin target gene expression. A molecular mechanism connecting the BRAF-hyperactivated MAPK and the physiological β -catenin pathway in the intestine may therefore depend partly on competing downstream transcriptional programs promoting progenitor TA versus ISC cellular states, respectively.

Although the intestinal epithelium is highly proliferative and has a rapid turnover, intestinal tumor progression is a long-term process. This suggests the existence of strong protective mechanisms limiting survival of cells that acquired oncogenic mutations in order to prohibit tumor initiation or progression. Mutational activation of BRAF elicits oncogene-induced senescence and apoptosis in melanoma.^{25,53,54} However, in agreement with another recent publication,¹⁸ we observed neither senescence nor apoptosis-related cleaved caspase3 in the intestine after oncogenic BRAF induction, although it has been reported before under similar conditions.²⁶ Strikingly, our data suggest the existence of a novel alternative fail-safe mechanism that may block tumor development after mutational activation of BRAF, that is, by oncogene-induced loss of stem cells. This mechanism could represent the prototype of a more general paradigm, as oncogene activities could possibly result in cellular signaling states incompatible with the maintenance of stem cell identity in other tissues, too, leading to discontinuation of the mutated cell progeny and clonal elimination. Further studies of oncogene-induced loss of stem cells could thus lead to new strategies to exploit colon cancer vulnerabilities.

MATERIALS AND METHODS

Mice

Transgene cassettes were constructed by linking tdTomato to human BRAF^{V600K} and/or murine stabilized mutant *Ctnnb1* (S33A, S37A, T41A and S45A) and/or firefly luciferase via 2A peptides, and subsequent cloning of these gene combinations into a doxycycline-inducible expression cassette flanked by wild-type and mutant loxP sites. Transgenes were integrated into the previously modified Gt(ROSA)26Sor locus of F1 hybrid B6/129S6 embryonic stem cells by Cre recombinase-mediated cassette exchange. Recombined embryonic stem cell clones were identified by Southern blotting, as described previously.²² Animals were generated by diploid aggregation. Previous experiments in adult mice have shown that this configuration results in high transgene induction in the intestinal epithelium, lower induction in some other tissues including skin and no discernible transgene expression in most tissues tested (data not shown). Mice were housed at a 12 h/12 h light/dark cycle and fed *ad libitum*. First- and second-generation transgenic mice with apparent 100% transgenic contribution were used for experiments (at least $n=4$ mice per genotype and time point). Transgenes were induced by administration of doxycycline (4 mg/ml) provided in a 1% sucrose solution via the drinking water. Primer sequences for genotyping are given in Supplementary Table 1. Termination criteria for the animal experiments were either weight loss or apparent distress, as indicated by a reduction of foraging activity or shivering. Animal experimentation was approved by Berlin authorities LAGeSo (G0185/09).

Organotypic culture

Organoid cultures were initiated and propagated as described in reference Sato *et al.*,³³ in 24-well or 48-well plates, using 15 or 30 μ l of Matrigel (BD, Heidelberg, Germany) per well. Crypt culture media were exchanged every other day, and cultures were passaged every 5–7 days. For all small-molecule inhibitors, maximal tolerated concentrations were determined in organoid culture in the absence of transgenic induction. The following inducers and small-molecule inhibitors were used: doxycycline (250 ng/ml, 500 ng/ml and 2 μ g/ml for weak, intermediary and strong transgene induction, respectively), PLX4720 (42 μ M), AZD6244 (8 μ M), GDC0941 (500 nM), CHIR99021 (6 μ M), Jagged1 (AnaSpec, Seraing, Belgium) and Wnt3a (Cell Signaling, Danvers, MA, USA) peptides were used at 1 μ M and 100 ng/ml, respectively. For signal inhibition experiments, doxycycline and small-molecule inhibitors were added at the same time, and wells were photographed 24, 36, 48 and 72 h after induction. Organoid survival was quantified from photographs, from at least three independent experiments.

Cell culture

Caco2-tet cells were tested to have no mutations in BRAF, KRAS, NRAS and MAP2K1 (own unpublished data). Cells were maintained in Dulbecco's modified Eagle's medium containing 10% fetal calf serum. Caco2-tet cells have previously been modified to express a second-generation tetracycline-regulated transactivator and transcriptional silencer.^{44,55} Caco2-tet were transfected using Lipofectamine 2000 (Life Technologies, Darmstadt, Germany) as per the manufacturer's instructions, using tetracycline-inducible plasmids coding for GFP, or combinations of GFP with BRAF^{V600E} or BRAF^{V600K}. We used luciferase reporter constructs with multimerized ELK, FOXO3 or LEF/TCF sites. Generally, 6 h after transfection, medium was exchanged to Dulbecco's modified Eagle's medium, 0.2% fetal calf serum and 2 μ g/ml doxycycline for induction. Cells were harvested 24–36 h after transfection. Reporter activity was measured using a dual-luciferase-assay (Life Technologies). FACS sorting of Caco2 cells for GFP expression was done using an Aria II sorter (BD).

IHC, RNA *in situ* hybridization, western analysis

For IHC and *in situ* hybridization, tissues were fixed in 4% formaldehyde, dehydrated via a graded ethanol series, embedded in paraffin and sectioned at 4 μ m. The following antibodies were used for IHC: anti-Ki67 (1:200; #ab16667 Abcam, Cambridge, UK), anti-RFP (1:200; #600-401-379 Rockland, Gilbertsville, PA, USA), anti-Lysozyme (1:200; #18-0039 Life Technologies), anti-ITF (1:100; Santa Cruz, Dallas, TX, USA), anti-phospho-MEK1/2 (1:100; #9121 Cell Signaling), anti-phospho-ERK1/2 (1:200; #9101 Cell Signaling). ImmPRESS secondary antibody and NovaRED substrate kits (Vector Labs, Burlingame, CA, USA) were used for IHC. *Olfm4 in situ* hybridization was carried out using standard protocols. Primer sequences

flanking the *in situ* probe are listed in Supplementary Table 1. DNA damage was detected by staining for γ H2AX, using the HCS DNA damage kit (Life Technologies), following the manufacturer's instructions. For SA- β -galactosidase staining, fresh tissues of induced and control mice were embedded in Tissue TEK (Sakura, Alphen, The Netherlands), snap-frozen and sectioned at 20 μ m on a cryostat. Sections were stained using the Senescence β -Galactosidase Kit (Cell Signaling), following the manufacturer's instructions.

For western analysis, purified intestinal epithelium or cell lines were lysed in sodium dodecyl sulfate lysis buffer and protein content was quantified by a BCA assay (Thermo Fisher, Waltham, MA, USA). Twenty or 40 μ g of protein lysates was separated on 12% polyacrylamide gels, and blotted onto nitrocellulose membranes. The following antibodies were used: anti-phospho-MEK1/2 (1:500; #9121 Cell Signaling), anti-phospho-ERK1/2 (1:500; #9101 Cell Signaling), anti-MEK1 (1:500; #9122 Cell Signaling), anti-ERK1/2 (1:500; #9102 Cell Signaling), RAF (1:200; #55522 Santa Cruz), anti-BRAF(V600E) (1:400; Spring Bioscience, Pleasanton, CA, USA), glyceraldehyde 3-phosphate dehydrogenase (1:10 000; #AM4300 Life Technologies). Alexa fluorophore-coupled secondary antibodies and an Odyssey scanner (Li-Cor, Bad Homburg, Germany) were used for visualization.

qRT-PCR and microarray analysis

For RNA analysis, villi were scraped from the inner intestinal surface after initial washing steps, whereas crypts were isolated by filtering (70 μ m, BD) after phosphate-buffered saline/EDTA treatment, as described in Sato *et al.*³³ For total tissue analysis, small pieces of the intestine were homogenized in Trizol (Life Technologies) using a Tissue Lyser machine (Qiagen, Hilden, Germany). Single-cell suspensions for FACS were prepared by digesting crypts of compound transgenic mice in 500 μ g/ml trypsin and 0.8 μ g/ml DNaseI for approximately 20 min at room temperature. Cells were microscopically examined for proper dissociation, washed and resuspended in Suspension Minimal Essential Medium (S MEM) (Life Technologies) containing DNaseI and subsequently filtered (30 μ m; Celltrics filter Partec, Münster, Germany). For FACS, an Aria SORP (BD) was used. For each profile, between 2000 and 20 000 cells were sorted directly into Qiagen buffer RLT containing 1% β -mercaptoethanol.

Total RNA was isolated from tissue and cell samples using RNeasy kits (Qiagen). Complementary DNA was synthesized from total RNA using the Transcriptor High Fidelity cDNA synthesis kit (Roche, Penzberg, Germany) as per the manufacturer's instructions. qRT-PCR was carried out using SYBR green (Promega, Mannheim, Germany) standard protocols. Relative expression was calculated using the $\Delta\Delta$ Ct method and *GAPDH* (human) or *Pmm2* (mouse) gene expression for normalization. qRT-PCR primer sequences are provided in Supplementary Table 1. *Lgr5* and *Ascl2* gene expression in BRAF^{V637E} mice was determined by Taqman qRT-PCR (Qiagen), as described in Rad *et al.*¹⁸ Gene expression profiling from FACS-sorted cell populations was done at AROS Applied Biotechnology (Aarhus, Denmark) using Illumina MouseRef-8 v2 chips and the NuGEN procedure for probe labeling. Expression data were calculated and normalized in Genome Studio GX 1.9 (Illumina, San Diego, CA, USA), using quantile normalization. Gene expression data were visualized using MultiExperiment Viewer (<http://www.tm4.org>). Gene set enrichment analysis was performed using pre-normalized Illumina gene expression data, following the authors guidelines.²⁸ Gene signatures and associated references are listed in Supplementary Table 2. Gene expression data are available in GEO under GSE50678.

CONFLICT OF INTEREST

The authors declare no conflict of interest.

ACKNOWLEDGEMENTS

This work was funded in part by NGFNplus grant PKM-01GS08105 to MM and BGH and eBio grant 0316184A to MM. We gratefully acknowledge Judith Seidemann (Charité Berlin), Gaby Bläß and Karol Macura (MPI-MG Berlin) for excellent technical assistance, Sonja Banko (animal facility, MPI-MG) for maintenance of the mice, Jan Dörr (Charité Berlin) for SA- β -Galactosidase stainings, Tilman Brummer (University of Freiburg) for the gift of Caco2-tet cells and Julian Heuberger (Max-Delbrück-Center for Molecular Medicine, Berlin) for the gift of the ITF antibody.

REFERENCES

- Barker N. Adult intestinal stem cells: critical drivers of epithelial homeostasis and regeneration. *Nat Rev Mol Cell Biol* 2013; **15**: 19–33.
- Sadanandam A, Lyssiotis CA, Homicsko K, Collisson EA, Gibb WJ, Wullschlegel S *et al*. A colorectal cancer classification system that associates cellular phenotype and responses to therapy. *Nat Med* 2013; **19**: 619–625.
- Fearon ER. Molecular genetics of colorectal cancer. *Annu Rev Pathol* 2011; **6**: 479–507.
- Takahashi M, Nakatsugi S, Sugimura T, Wakabayashi K. Frequent mutations of the beta-catenin gene in mouse colon tumors induced by azoxymethane. *Carcinogenesis* 2000; **21**: 1117–1120.
- Su LK, Kinzler KW, Vogelstein B, Preisinger AC, Moser AR, Luongo C *et al*. Multiple intestinal neoplasia caused by a mutation in the murine homolog of the APC gene. *Science* 1992; **256**: 668–670.
- Niehrs C. The complex world of WNT receptor signalling. *Nat Rev Mol Cell Biol* 2012; **13**: 767–779.
- van de Wetering M, Sancho E, Verweij C, de Lau W, Oving I, Hurlstone A *et al*. The beta-catenin/TCF-4 complex imposes a crypt progenitor phenotype on colorectal cancer cells. *Cell* 2002; **111**: 241–250.
- van Es JH, Haegbarth A, Kujala P, Itzkovitz S, Koo B-K, Boj SF *et al*. A critical role for the Wnt effector Tcf4 in adult intestinal homeostatic self-renewal. *Mol Cell Biol* 2012; **32**: 1918–1927.
- Farrall AL, Riemer P, Leushacke M, Sreekumar A, Grimm C, Herrmann BG *et al*. Wnt and BMP signals control intestinal adenoma cell fates. *Int J Cancer* 2012; **131**: 2242–2252.
- Snover DC. Update on the serrated pathway to colorectal carcinoma. *Hum Pathol* 2011; **42**: 1–10.
- Bettington M, Walker N, Clouston A, Brown I, Leggett B, Whitehall V. The serrated pathway to colorectal carcinoma: current concepts and challenges. *Histopathology* 2013; **62**: 367–386.
- Laiho P, Kokko A, Vanharanta S, Salovaara R, Sammalkorpi H, Järvinen H *et al*. Serrated carcinomas form a subclass of colorectal cancer with distinct molecular basis. *Oncogene* 2007; **26**: 312–320.
- Osaki LH, Gama P. MAPKs and signal transduction in the control of gastrointestinal epithelial cell proliferation and differentiation. *Int J Mol Sci* 2013; **14**: 10143–10161.
- Cancer Genome Atlas Network. Comprehensive molecular characterization of human colon and rectal cancer. *Nature* 2012; **487**: 330–337.
- Lao VV, Grady WM. Epigenetics and colorectal cancer. *Nat Rev Gastroenterol Hepatol* 2011; **8**: 686–700.
- Wu JM, Montgomery EA, Iacobuzio-Donahue CA. Frequent beta-catenin nuclear labeling in sessile serrated polyps of the colon with neoplastic potential. *Am J Clin Pathol* 2008; **129**: 416–423.
- Yachida S, Mudali S, Martin SA, Montgomery EA, Iacobuzio-Donahue CA. Beta-catenin nuclear labeling is a common feature of sessile serrated adenomas and correlates with early neoplastic progression after BRAF activation. *Am J Surg Pathol* 2009; **33**: 1823–1832.
- Rad R, Cadiñanos J, Rad L, Varela I, Strong A, Kriegl L *et al*. A genetic progression model of BraF(V600E)-induced intestinal tumorigenesis reveals targets for therapeutic intervention. *Cancer Cell* 2013; **24**: 15–29.
- El-Osta H, Falchok G, Tsimberidou A, Hong D, Naing A, Kim K *et al*. BRAF mutations in advanced cancers: clinical characteristics and outcomes. *PLoS ONE* 2011; **6**: e25806.
- Wan P, Garnett MJ, Roe SM, Lee S, Niculescu-Duvaz D, Good VM *et al*. Mechanism of activation of the RAF-ERK signaling pathway by oncogenic mutations of B-RAF. *Cell* 2004; **116**: 855–867.
- Brunet A, Bonni A, Zigmond MJ, Lin MZ, Juo P, Hu LS *et al*. Akt promotes cell survival by phosphorylating and inhibiting a Forkhead transcription factor. *Cell* 1999; **96**: 857–868.
- Vidigal JA, Morkel M, Wittler L, Brouwer-Lehmitz A, Grote P, Macura K *et al*. An inducible RNA interference system for the functional dissection of mouse embryogenesis. *Nucleic Acids Res* 2010; **38**: e122.
- Muñoz J, Stange DE, Schepers AG, van de Wetering M, Koo B-K, Itzkovitz S *et al*. The *Lgr5* intestinal stem cell signature: robust expression of proposed quiescent “+4” cell markers. *EMBO J* 2012; **31**: 3079–3091.
- Barker N, van Es JH, Kuipers J, Kujala P, van den Born M, Cozijnsen M *et al*. Identification of stem cells in small intestine and colon by marker gene *Lgr5*. *Nature* 2007; **449**: 1003–1007.
- Wajapeyee N, Serra RW, Zhu X, Mahalingam M, Green MR. Oncogenic BRAF induces senescence and apoptosis through pathways mediated by the secreted protein IGFBP7. *Cell* 2008; **132**: 363–374.
- Carragher LAS, Snell KR, Giblett SM, Aldridge VSS, Patel B, Cook SJ *et al*. V600EBraf induces gastrointestinal crypt senescence and promotes tumour progression through enhanced CpG methylation of p16INK4a. *EMBO Mol Med* 2010; **2**: 458–471.

- 27 Gonzalo DH, Lai KK, Shadrach B, Goldblum JR, Bennett AE, Downs-Kelly E *et al*. Gene expression profiling of serrated polyps identifies annexin A10 as a marker of a sessile serrated adenoma/polyp. *J Pathol* 2013; **230**: 420–429.
- 28 Subramanian A, Tamayo P, Mootha VK, Mukherjee S, Ebert BL, Gillette MA *et al*. Gene set enrichment analysis: a knowledge-based approach for interpreting genome-wide expression profiles. *Proc Natl Acad Sci USA* 2005; **102**: 15545–15550.
- 29 Jürchott K, Kuban R-J, Krech T, Blüthgen N, Stein U, Walther W *et al*. Identification of Y-box binding protein 1 as a core regulator of MEK/ERK pathway-dependent gene signatures in colorectal cancer cells. *PLoS Genet* 2010; **6**: e1001231.
- 30 Azzolin L, Zanconato F, Bresolin S, Forcato M, Basso G, Bicciato S *et al*. Role of TAZ as mediator of Wnt signaling. *Cell* 2012; **151**: 1443–1456.
- 31 Van der Flier L, Sabates Bellver J, Oving I. The intestinal Wnt/TCF signature. *Gastroenterology* 2007; **132**: 628–632.
- 32 Merlos-Suárez A, Barriga FM, Jung P, Iglesias M, Céspedes MV, Rossell D *et al*. The intestinal stem cell signature identifies colorectal cancer stem cells and predicts disease relapse. *Cell Stem Cell* 2011; **8**: 511–524.
- 33 Sato T, Stange DE, Ferrante M, Vries RGJ, van Es JH, van den Brink S *et al*. Long-term expansion of epithelial organoids from human colon, adenoma, adenocarcinoma, and Barrett's epithelium. *Gastroenterology* 2011; **141**: 1762–1772.
- 34 Farin HF, van Es JH, Clevers H. Redundant sources of wnt regulate intestinal stem cells and promote formation of paneth cells. *Gastroenterology* 2012; **143**: e7.
- 35 Tsai J, Lee JT, Wang W, Zhang J, Cho H, Mamo S *et al*. Discovery of a selective inhibitor of oncogenic B-Raf kinase with potent antimelanoma activity. *Proc Natl Acad Sci USA* 2008; **105**: 3041–3046.
- 36 Yeh TC, Marsh V, Bernat BA, Ballard J, Colwell H, Evans RJ *et al*. Biological characterization of ARRY-142886 (AZD6244), a potent, highly selective mitogen-activated protein kinase kinase 1/2 inhibitor. *Clin Cancer Res* 2007; **13**: 1576–1583.
- 37 Folkes AJ, Ahmadi K, Alderton WK, Alix S, Baker SJ, Box G *et al*. The identification of 2-(1H-indazol-4-yl)-6-(4-methanesulfonyl-piperazin-1-ylmethyl)-4-morpholin-4-yl-thieno[3,2-d]pyrimidine (GDC-0941) as a potent, selective, orally bioavailable inhibitor of class I PI3 kinase for the treatment of cancer. *J Med Chem* 2008; **51**: 5522–5532.
- 38 Murray JT, Campbell DG, Morrice N, Auld GC, Shpiro N, Marquez R *et al*. Exploitation of KESTREL to identify NDRG family members as physiological substrates for SGK1 and GSK3. *Biochem J* 2004; **384**: 477–488.
- 39 Ying Q-L, Wray J, Nichols J, Batlle-Morera L, Doble B, Woodgett J *et al*. The ground state of embryonic stem cell self-renewal. *Nature* 2008; **453**: 519–523.
- 40 Kimura T, Yamamoto E, Yamano H-O, Suzuki H, Kamimae S, Nojima M *et al*. A novel pit pattern identifies the precursor of colorectal cancer derived from sessile serrated adenoma. *Am J Gastroenterol* 2012; **107**: 460–469.
- 41 Little AS, Balmanno K, Sale MJ, Newman S, Dry JR, Hampson M *et al*. Amplification of the driving oncogene, KRAS or BRAF, underpins acquired resistance to MEK1/2 inhibitors in colorectal cancer cells. *Sci Signal* 2011; **4**: ra17.
- 42 Corcoran RB, Dias-Santagata D, Bergethon K, Iafrate AJ, Settleman J, Engelman JA. BRAF gene amplification can promote acquired resistance to MEK inhibitors in cancer cells harboring the BRAF V600E mutation. *Sci Signal* 2010; **3**: ra84.
- 43 Pylayeva-Gupta Y, Grabocka E, Bar-Sagi D. RAS oncogenes: weaving a tumorigenic web. *Nat Rev Cancer* 2011; **11**: 761–774.
- 44 Fritsche-Guenther R, Witzel F, Sieber A, Herr R, Schmidt N, Braun S *et al*. Strong negative feedback from Erk to Raf confers robustness to MAPK signalling. *Mol Syst Biol* 2011; **7**: 489.
- 45 Bennecke M, Kriegl L, Bajbouj M, Retzlaff K, Robine S, Jung A *et al*. Ink4a/Arf and oncogene-induced senescence prevent tumor progression during alternative colorectal tumorigenesis. *Cancer Cell* 2010; **18**: 135–146.
- 46 Schwitalla S, Fingerle AA, Cammareri P, Nebelsiek T, Göktuna SI, Ziegler PK *et al*. Intestinal tumorigenesis initiated by dedifferentiation and acquisition of stem-cell-like properties. *Cell* 2012; **152**: 25–38.
- 47 Vermeulen L, Morrissey E, van der Heijden M, Nicholson AM, Sottoriva A, Buczacchi S *et al*. Defining stem cell dynamics in models of intestinal tumor initiation. *Science* 2013; **342**: 995–998.
- 48 Moon B-S, Jeong W-J, Park J, Kim TI, Min DS, Choi K-Y. Role of oncogenic K-Ras in cancer stem cell activation by aberrant Wnt/ β -catenin signaling. *J Natl Cancer Inst* 2014; **106**: djt373.
- 49 Phelps RA, Chidester S, Dehghanizadeh S, Phelps J, Sandoval IT, Rai K *et al*. A two-step model for colon adenoma initiation and progression caused by APC loss. *Cell* 2009; **137**: 623–634.
- 50 Jeong W-J, Yoon J, Park J-C, Lee S-H, Lee S-H, Kaduwal S *et al*. Ras stabilization through aberrant activation of Wnt/ β -catenin signaling promotes intestinal tumorigenesis. *Sci Signal* 2012; **5**: ra30.
- 51 Biechele TL, Kulikauskas RM, Toroni RA, Lucero OM, Swift RD, James RG *et al*. Wnt/ β -catenin signaling and AXIN1 regulate apoptosis triggered by inhibition of the mutant kinase BRAFV600E in human melanoma. *Sci Signal* 2012; **5**: ra3.
- 52 Guardavaccaro D, Clevers H. Wnt/ β -catenin and MAPK signaling: allies and enemies in different battlefields. *Sci Signal* 2012; **5**: pe15.
- 53 Michaloglou C, Vredeveld LCW, Soengas MS, Denoyelle C, Kuilman T, van der Horst CMAM *et al*. BRAF600-associated senescence-like cell cycle arrest of human naevi. *Nature* 2005; **436**: 720–724.
- 54 Dhomen N, Reis-Filho JS, da Rocha Dias S, Hayward R, Savage K, Delmas V *et al*. Oncogenic Braf induces melanocyte senescence and melanoma in mice. *Cancer Cell* 2009; **15**: 294–303.
- 55 Herr R, Wöhrlé FU, Danke C, Berens C, Brummer T. A novel MCF-10A line allowing conditional oncogene expression in 3D culture. *Cell Commun Signal* 2011; **9**: 17.

Supplementary Information accompanies this paper on the Oncogene website (<http://www.nature.com/onc>)